



Biomethane and propylene glycol synthesis via a novel integrated catalytic transfer hydrogenolysis, carbon capture and biomethanation process

Jude A. Okolie^{a,*}, Fredrick O. Omoarukhe^b, Emmanuel I. Epelle^c, Chukwuma C. Ogbaga^d, Adekunle A. Adeleke^e, Patrick U. Okoye^f

^a Gallogly College of Engineering, University of Oklahoma, Norman, OK, United States

^b Department of Chemical Engineering, University of Ilorin, P. M. B. 1515, Ilorin, Nigeria

^c School of Computing, Engineering & Physical Sciences, University of the West of Scotland, Paisley PA1 2BE, United Kingdom

^d Independent Researcher, Middlesbrough, North Yorkshire, United Kingdom

^e Department of Mechanical Engineering, Nile University of Nigeria, Airport Road, Abuja, Nigeria

^f Instituto de Energías Renovables (IER-UNAM), Privada Xochicalco s/n Col, Centro, Temixco, Morelos 62580, Mexico

ARTICLE INFO

Keywords:

Biomethane
Propylene glycol
Techno-economic analysis
Simulation
Glycerol

ABSTRACT

A novel conceptual design for the co-production of biomethane and propylene glycol from integrated catalytic transfer hydrogenolysis (CTH), biogenic CO₂ capture and biomethanation reaction was presented in this study. Furthermore, process economics and environmental impact study was performed to appraise the feasibility of the proposed design. The minimum selling price (MSP) of propylene glycol produced considering the overall cost of biomethane as co-product is 1.41 U.S.\$/kg. However, if the cost of biomethane was not considered or if the biomethane produced is not enough to yield a yearly revenue then the MSP would increase to 1.43 U.S.\$/kg. The MSP of biomethane for the integrated process was 148 U.S.\$/MWh. The MSPs of propylene glycol and biomethane were comparable with those of the business-as-usual technology. Factors such as hydrogen donor solvent cost, catalyst cost, electricity price and equipment purchase cost influenced the MSP. Environmental assessment studies showed that the standalone CTH had a higher overall carbon footprint (carbon emissions of 3.7 MM tonnes/yr.). This could be attributed to the consumption of CO₂ derived from the process streams via biomethanation process.

Abbreviations

aspen process economic analyzer APEA
business as usual BAU
capital expenditure CAPEX
catalytic transfer hydrogenolysis CTH
discounted cash flow analysis DCFA
equation of state EOS
equipment purchase costs EPC
fixed operating cost FOC
life cycle assessment LCA
minimum selling price MSP
monoethanolamine MEA
net present value NPV
non-random two-liquid -Redlich-Kwong NRTL-RK
operating expenditure OPEX

renewable heat incentives RHI
startup cost SUC
techno-economic analysis TEA
vacuum-temperature swing adsorption cycle VTSA
variable operating cost VOC

1. Introduction

The increasing depletion of petroleum resources coupled with the environmental concerns associated with their consumption has led to an interest in alternative and sustainable energy resources. Biodiesel is seen as a very good alternative to conventional petroleum fuels for the transportation industry due to its environmentally benign nature including net zero carbon dioxide emission and fewer releases of SO_x and NO_x-containing compounds. Pure biodiesel or blends with petroleum-derived diesel in various weight fractions can be used as fuel

* Corresponding author.

E-mail address: Jude.okolie@ou.edu (J.A. Okolie).

<https://doi.org/10.1016/j.cej.2023.100523>

for vehicles, furnaces, stationary equipment, and engines. Some researchers have investigated the use of biodiesel as a fuel for aviation turbo engines [1].

Biodiesel can be produced from several pathways such as micro-emulsions, pyrolysis, transesterification reaction, and direct use of pure vegetable oils or blending with petroleum diesel [2]. Among the several production methods, transesterification is one of the established technology. Transesterification occurs when vegetable oils or animal fats react with alcohols in the presence of a catalyst [3]. Although promising, the process produces lots of crude glycerol as a by-product. It has been experimentally proven that every 9 kg of biodiesel production also yields 1 kg of crude glycerol [4]. About 80% of crude glycerol contains glycerol and impurities such as soaps and methanol, inorganic elements, and fatty acid methyl esters (FAMES) [2]. Moreover, crude glycerol requires expensive separation methods that limit its commercial value. On the other hand, if crude glycerol is converted to value-added chemicals through an integrated biorefinery the profitability of biodiesel production could be increased.

Crude glycerol can be converted to biofuels and several value-added chemicals such as ethanol; D-lactic acid; 1,2-propanediol, poly-3-hydroxybutyrate, and succinic acid. Propylene glycol, also known as 1,2-propanediol, is a promising chemical with many applications, including as an antifreeze, moisturizer, solvent, cosmetics, agent, preservative, and surfactant [5]. It can be synthesized from glycerol via a catalyst-aided selective hydrogenolysis reaction [6]. In contrast to commercial processes like the hydrolysis of propylene oxide generated from petroleum, the conversion of glycerol to renewable propylene glycol offers a sustainable route. However, the production of propylene glycol from the catalytic hydrogenolysis of glycerol faces several challenges including high-pressure hydrogen requirement, product separation complexity, catalyst selection and recovery as well as high reaction temperature [6].

To address the limitation of catalytic hydrogenolysis, several studies have explored the catalytic transfer hydrogenolysis method (CTH) for converting glycerol to propylene glycol [7]. The process requires lower temperature and pressure and occurs without the addition of external hydrogen [8]. During CTH, reductive organic molecules such as ethanol, methanol and formic acid are used as in-situ hydrogen donors [9]. Previous studies have demonstrated the advantages of CTH over catalytic hydrogenolysis in terms of improved energy efficiency and profitability [8]. However, CTH produces several by-products that are difficult to separate, and sometimes require expensive separation methods. Therefore, it is imperative to develop integrated processes that combine CTH with other green chemical production processes to promote material utilization, minimize the cost of standalone processes and eliminate or reduce the process' environmental impacts. Furthermore, the integration of CTH with other biomass conversion processes could also provide an alternative pathway for the generation of other value-added products.

The conversion of glycerol to biofuels and value-added products has been investigated in several research using various integrated methods. Okolie et al. [10] proposed an integrated process for the co-production of bioethanol and biomethane from crude glycerol. The process combines hydrothermal gasification and biomethanation product. The authors reported a minimum bioethanol selling price of USD 1.4 per liter for the process. Supramono and Ashshiddiq. [11] developed a process for the co-production of acrolein and propylene. The process yielded a net present value (NPV), internal rate of return, and payback period of USD 376 million, 149.9%, 1.26 years and 149.9% respectively. In another study, Sun et al. [8] explored the economic feasibility of the catalytic hydrogenolysis process and compared the results with CTH. The latter was preferable in terms of economic and environmental impacts. It should be mentioned that there are relatively few studies on the process simulation of CTH despite the promising experimental reports documented in previous studies. In addition, an integrated process that combined CTH with other technology for the co-production of different

value-added products is scarcely documented. To address the knowledge gaps the present study proposes a conceptual design to produce propylene glycol and biomethane via an integrated CTH and biomethanation reaction. To determine whether the suggested design is economically viable, a thorough techno-economic analysis is conducted. Another novelty of the study is the development of process models for CTH, CO₂ capture and biomethanation reaction. The model is relevant for process optimization, techno-economic analysis (TEA), and life cycle assessment (LCA).

2. Methodology

The present study designed and modeled the co-production of propylene glycol and biomethane from CTH of glycerol with CO₂ capture and biomethanation reaction. Propylene glycol production was modeled via CTH of glycerol [10]. Liquid ethanol was used as an in-situ hydrogen donor. Ethanol was selected as a hydrogen donor because it has been experimentally proven to supply sufficient in-situ hydrogen by several researchers [12,13]. The integrated process also includes CO₂ capture and biomethanation reaction. It should be mentioned that some of the hydrogen produced from the CTH is separated from the gaseous product and used for the biomethanation reaction. Fig. 1 shows the overall process flow diagram of the conceptual design.

2.1. Process design

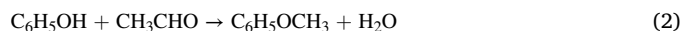
2.1.1. Catalytic transfer hydrogenolysis unit

The process simulation of CTH of glycerol to produce propylene glycol was performed with Aspen Plus® V10 and MATLAB as shown in Fig. 1a. Detailed information about the steps required for developing the Aspen Plus-MATLAB subroutines algorithm can be found elsewhere [14, 15]. In the case of a CTH process, the integration can be achieved by developing a custom Aspen Plus model that calls a MATLAB script for the calculation of kinetic rate parameters. This ensures the simulation of complex reaction mechanisms and the optimization of process variables using MATLAB's optimization tools. The MATLAB script was embedded within Aspen Plus using a custom unit operation and a user-defined kinetic model. Detailed information about the equations used is provided in Eqs. (1)–(6).

Ethanol dehydrogenation:



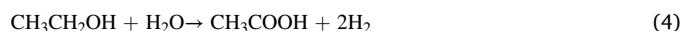
Hydrogen transfer from ethanol to phenol:



Hydrogenolysis of the intermediate:



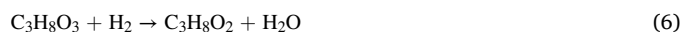
The reaction of ethanol with water



Glycerol decomposition:



Glycerol hydrogenolysis to produce



Ethylene glycol formation



Glycerol hydration



The NRTL-RK equation of state (EOS) was selected for the phase

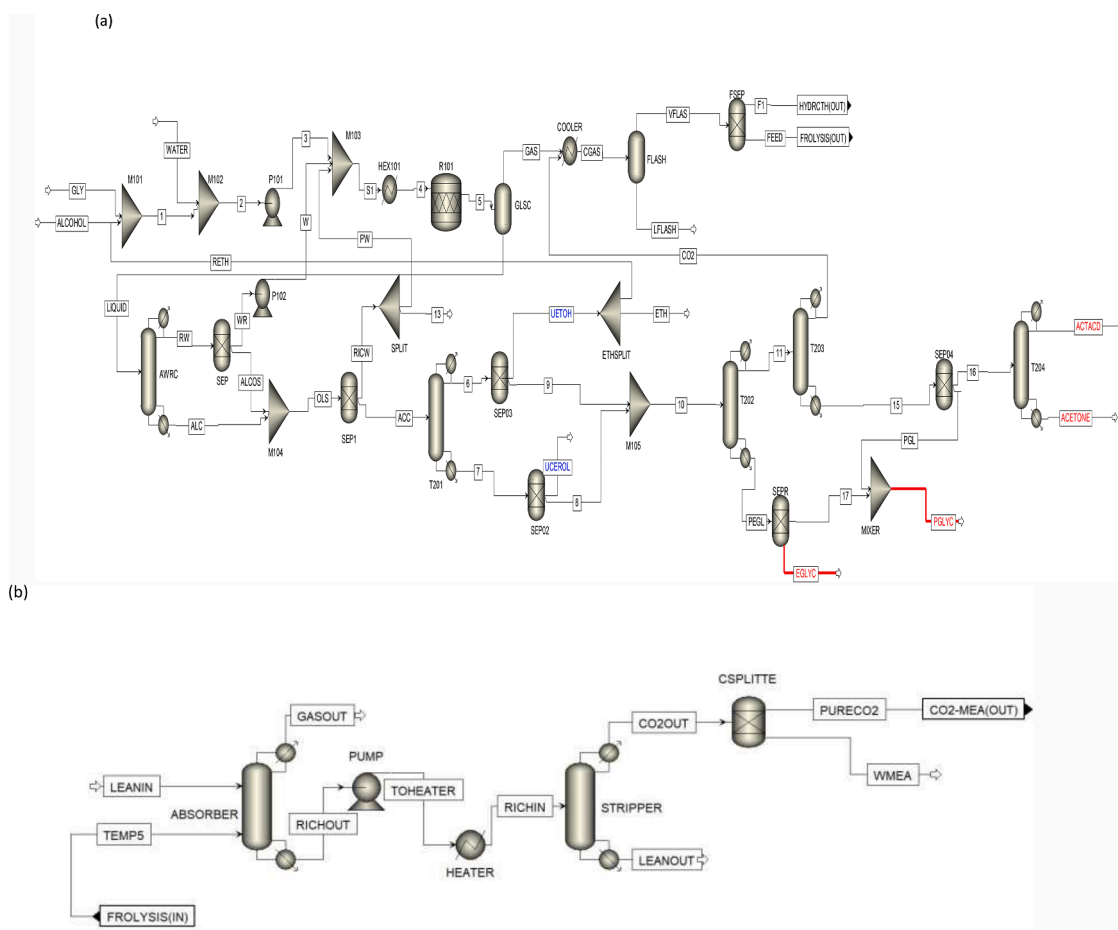


Fig. 1. Process flow diagram of (a) catalytic transfer hydrogenolysis (b) CO₂ MEA absorption process unit in Aspen Plus.

equilibrium estimation because it is appropriate for polar and gas-liquid phase systems [8]. The feed stream used was pure glycerol (100 wt.%), ethanol (serves as hydrogen donor), and water mixed in a ratio of 1:1:0.4. The feed was pumped and preheated at 0.14 MPa and 150 °C and fed to the reactor (R101). The reactor operates at a temperature of 180 °C and 1.8 MPa. It is important to note that the operating conditions of the reactor were specified based on a previous experimental report [9]. Moreover, CTH occurs at milder reaction temperatures (<200 °C) and pressure (<2 MPa) [16].

The R101 block representing the CTH reactor was with a stoichiometric block in Aspen Plus. The stoichiometric block takes the user's input, including the feed composition and process conditions, and calculates the theoretical reaction stoichiometry based on the chemical equations. It also calculates the heat of the reaction and the reactant and product flow rates based on the reaction stoichiometry. Eqs. (1)–(7) are used to model the stoichiometric block in Aspen Plus.

The reactor effluents which contain mostly water, hydrogen, propylene glycol, carbon dioxide, and other value-added products were sent to a gas-liquid separator where the gas components are flashed. After which the liquid components were fed to a series of distillation columns for efficient recovery of several products including propylene glycol, methanol, acetol and acetic acid, and ethylene glycol. Furthermore, the dissolved gasses, unreacted glycerol, and water were recycled back as feed to ensure maximum product recovery and resource management. It should be mentioned that the distillation column was modeled by implementing a series of RadFrac combinations in Aspen Plus. The number of stages and the reflux ratio are determined by using the trial-and-error method. The number of stages used in each distillation column can be found in Table S2 of the supplementary materials. The columns were designed with assumptions of constant molar overflow and

constant relative volatility between light and heavy keys. The selection of the number of stages through the trial-and-error method involves changing the number of stages and observing the impact on product purity. Once a product purity of more than 90 percent was obtained the subsequent number of stages was selected. Then the column operating parameters including the reflux ratio, reboiler and condenser duty were selected by letting Aspen Plus calculate them by using product purity. It should be mentioned that the rigorous trial and error method was selected over the shortcut method because it is more detailed and provides an accurate estimation of the number of stages. While the shortcut method is restricted to ideal mixtures and total condensation or reboil, the rigorous method can handle non-ideal mixtures as well as partial condensations [17].

The gas stream obtained from the gas-liquid separation was cooled and further sent to MEA-CO₂ capture unit for CO₂ recovery. Aspen Plus modeling description of the MEA-CO₂ capture unit is presented in the next section.

2.1.2. CO₂ capture unit

Several technologies such as membrane separation, liquid scrubbing, and vacuum-temperature swing adsorption cycle (VTSA) processes have been employed for the direct capture of CO₂ from gas streams as a pathway to decarbonize energy systems and achieve net-zero emissions [18]. Among these technologies, liquid scrubbing is considered the benchmark for CO₂ capture and has been considered in hundreds of gas separation processes due to the inexpensive cost of components [19,20]. The liquid scrubbing processes are mainly divided into namely: alkaline scrubbing and amine scrubbing processes. For this study, the use of aqueous monoethanolamine (MEA) was employed for CO₂ capture due to its fast absorption rate and because it is a commercially matured

technology [21]. Furthermore, the MEA-CO₂ absorption process has been successfully implemented by several researchers for the efficient capture of CO₂ from flue gas [22–24]. MEA also have a relatively low cost, is readily available, and has a high CO₂ capture capacity.

The MEA-CO₂ absorption process, which is a continuous process involves providing a simpler contact between the gas streams and MEA. The contact leads to subsequent absorption and stripping/desorption.

Modeling of MEA – CO₂ absorption involves a detailed description of each chemical reaction inherent in the process. Table 1 shows the electrolyte chemistry solution of the MEA-CO₂-H₂O via the dissociation of ions. The gas stream was contacted with lean-MEA in a column for absorbing CO₂. The rich-MEA solvent stream, after absorbing CO₂, was pumped to the stripper, and preheated by the lean/rich heat exchanger before being fed into a column for the desorption process to occur and for the rich-MEA stream to be regenerated. A conventional packed column (RADFRAC) was used for CO₂ absorption using a 30 wt.% MEA solution.

A rigorous, rate-based MEA thermodynamic model was utilized for CO₂ capture based on the template available in Aspen process simulator as shown in Fig. 1b. The fluid package, NRTL-RK, was used for estimating the liquid and vapor properties such as entropy, activity coefficient, enthalpy, and fugacity coefficients [26]. The Aspen Plus unit blocks description used for the modeling is shown in Table S1 in the supplementary materials.

The CO₂ capture unit template facilitates the modeling and simulation of carbon capture processes, utilizing various technologies such as absorption, adsorption, and membranes to separate CO₂ from process gas streams. Although MEA absorption process was selected in the present study. The template streamlines the setup and analysis of CO₂ capture systems, allowing users to quickly evaluate the performance, efficiency, and cost-effectiveness of different configurations and operating conditions. By leveraging the robust thermodynamic models and unit operations within Aspen Plus simulator, the CO₂ capture unit template provides a valuable tool for engineers and researchers working on the design, optimization, and integration of carbon capture solutions in various industries to mitigate greenhouse gas emissions and address climate change challenges.

2.1.3. Biomethane production unit

The renewable hydrogen obtained from the catalytic transfer hydrogenolysis unit and pure CO₂ captured from the MEA-CO₂ removal process were utilized to produce biomethane. The hydrogenation of CO₂ for biomethane production can proceed via biological synthesis or thermochemical reaction [27]. However, for this study, biological synthesis was utilized because the microorganisms used as biocatalysts have a high tolerance for the impurities that are typically found in the biomethanation feed gas [10]. Furthermore, biological biomethane production occurs at a lower temperature compared to the thermochemical process.



For this study, the biomethanation reactor was modeled using an RStoic reactor which operates at mesophilic conditions of 60 °C and 5 bar, with a CO₂ conversion of 98.6% and a stoichiometric ratio of H₂/

Table 1
Chemical reactions in the MEA-CO₂-H₂O [25].

No.	Type	Reactions
1	Equilibrium	$2\text{H}_2\text{O} \leftrightarrow \text{H}_3\text{O}^+ + \text{OH}^-$
2	Equilibrium	$\text{CO}_2 + 2\text{H}_2\text{O} \leftrightarrow \text{H}_3\text{O}^+ + \text{HCO}_3^-$
3	Equilibrium	$\text{HCO}_3^- + \text{H}_2\text{O} \leftrightarrow \text{CO}_3^{2-} + \text{H}_3\text{O}^+$
4	Equilibrium	$\text{MEA} + \text{H}_3\text{O}^+ \leftrightarrow \text{MEAH}^+ + \text{H}_2\text{O}$
5	Kinetic	$\text{O}_2 + \text{OH}^- \rightarrow \text{HCO}_3^-$
6	Kinetic	$\text{HCO}_3^- \rightarrow \text{CO}_2 + \text{OH}^-$
7	Kinetic	$\text{MEA} + \text{CO}_2 + \text{H}_2\text{O} \rightarrow \text{MEACOO}^- + \text{H}_3\text{O}^+$
8	Kinetic	$\text{MEACOO}^- + \text{H}_3\text{O}^+ \rightarrow \text{MEA} + \text{CO}_2 + \text{H}_2\text{O}$

CO₂ of 1:4 as shown in Eq. (10) [10]. Additionally, because of the reactor's exothermic nature, the reactor employed was a jacketed reactor, which uses circulating water to maintain isothermal conditions.

The concept of adding an integrated CO₂ capture and biomethanation process to produce biomethane could have several benefits and industrial relevance. Utilizing the waste CO₂ for biofuel production provides a potential cost savings benefit. Both CO₂ capture and hydrogenation technologies are established and widely used in industry. This means that the technology needed to implement an integrated CO₂ capture and biomethanation process already exists and has been proven effective. By capturing waste CO₂ and converting it to biomethane through hydrogenation, the integrated process has the potential to produce energy that is carbon-neutral or even carbon-negative. This could be an attractive option for companies and governments that are looking to reduce their carbon footprint and meet climate change targets. The integrated process could potentially be more efficient than standalone CO₂ capture and biomethanation processes since the waste CO₂ is being used as a feedstock for the biomethanation process. This could result in lower overall costs and improved environmental performance.

2.2. Economic evaluation

Since there is no data for commercial-scale production, it is important that we explore the TEA of the conceptual process design. This is crucial for determining the minimum selling price (MSP) of biomethane and propylene glycol produced. In addition, presenting a comprehensive economic model for the conceptual process design will assist in creating an investment climate that will foster technological change in today's volatile market and serve as a guideline for the commercialization of a plant that produces propylene glycol. For this study, various economic indicators such as OPEX (Operating Expenditure), NPV (Net Present Value), CAPEX (Capital Expenditure), and Minimum selling price (MSP) were used to assess the feasibility of this conceptual process design [28].

The total of all discounted cash flows, or present values of all cash flows, including the initial investment at the time of analysis, is known as the net present value, or NPV. The MSP, in contrast, is described as the price that generates zero NPV. The NPV was assessed using discounted cash flow analysis (DCFA). The equipment purchase costs (EPC) were calculated using the Aspen Process Economic Analyzer (APEA) and a literature search. With APEA, the cost of heat exchangers for the entire plant was also calculated. Using the chemical engineering plant cost indices (CEPCI), all anticipated costs were scaled up to 2022. A CEPCI of 801.3 for the year 2022 was used in the study [29]. The percentage of the EPC was used to compute the CAPEX. In the same manner, the OPEX was determined based on the assumptions outlined in our previous studies [30,10].

3. Results and discussions

3.1. Product distribution, mass balance and energy analysis

Fig. 2 shows the material balance from all the key process operations including the CTH and biomethanation units. It should be mentioned that the mass balance results were presented at a pressure of 2 MPa and temperature of 220 °C respectively and a 1:1 glycerol to ethanol ratio. Also, these optimum reaction conditions were selected based on previous experimental results [31–33]. The mass balance shows the formation of 110 kg/hr methane and 2425 kg/hr propylene glycol for every 5000 kg/hr of glycerol. The process also requires an ethanol hydrogen donor and water of 5000 kg/hr and 2000 kg/hr respectively. About 1000 kg/hr of CO₂ was produced and converted to biomethane via biomethanation reaction. The propylene glycol selectivity and glycerol conversion yield are reported as 48.48% and 90.22% respectively. The product distribution shown in Fig. 2 indicates that almost 46% of the major liquid products are propylene glycol. While key products such as

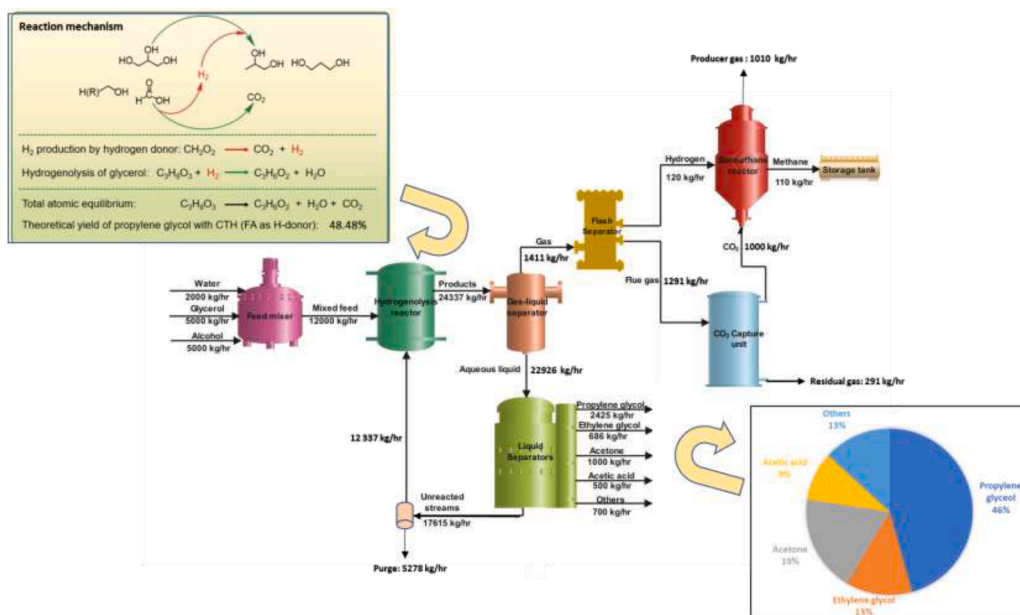


Fig. 2. Schematics of the mass balance of catalytic transfer hydrogenolysis including the product distribution and biomethane production.

acetone, ethylene glycol, acetic acid and aqueous organics are produced in small quantities. Based on the simulation results for mass and energy flows of different products during CTH as well as literature reports, a reaction mechanism was proposed for CTH and presented in Fig. 2. The ethanol hydrogen donor spills active hydrogen species on the catalyst’s surface during a reaction to promote a hydrogenolysis reaction [34]. The dual active site catalysts also contain the site that promotes the reaction of hydrogen with glycerol leading to the formation of several products including propylene glycol and lower alcohols.

The glycerol conversion yield presented herein is in close agreement with previously reported modeling values. For instance, Jiménez et al. [5] reported a glycerol conversion of 98.2% during the hydrogenolysis of glycerol at temperature and pressure of 220 °C and 4 MPa respectively and hydrogen to glycerol molar ratio of 5:1 with Aspen Hysys simulation. Gonzalez-Garay et al. [35] observed glycerol conversion and propylene glycol selectivity of 96% and 33%, respectively at 240 °C temperature and pressure of 2 MPa with 50 wt.% feed concentration with Aspen Plus simulation. Some experimental studies have also

reported a glycerol conversion similar to the simulated results as presented in Fig. 3 [31,32,34]. Yuan et al. [36] used a Cu/ZnO – Al₂O₃ enhanced catalyst for the CTH of glycerol with glycerol aqueous solution as hydrogen donor. The authors reported 95.6% glycerol conversion and 51.3% propylene glycol selectivity. In another study, Cu/MgAlO catalyzed CTH in the presence of ethanol hydrogen donor produced higher glycerol conversion and propylene glycol selectivity of 95.1% and 92.2% respectively [37]. Based on the observations in Fig. 3, glycerol conversion from the proposed model is in close agreement with experimental results. However, a large deviation exists in the propylene glycol selectivity. This deviation could be because of the amount and nature of the catalyst used among different authors. Additionally, the type of reactor and different hydrogen donor agents such as ethanol, methanol or formic acid could impact the product yield and selectivity. Regardless, the model results presented herein are valid for further economic appraisal of the conceptual design.

Fig. 4 shows the schematics for the energy balance for the entire process. As outlined earlier, the entire process involves the production of

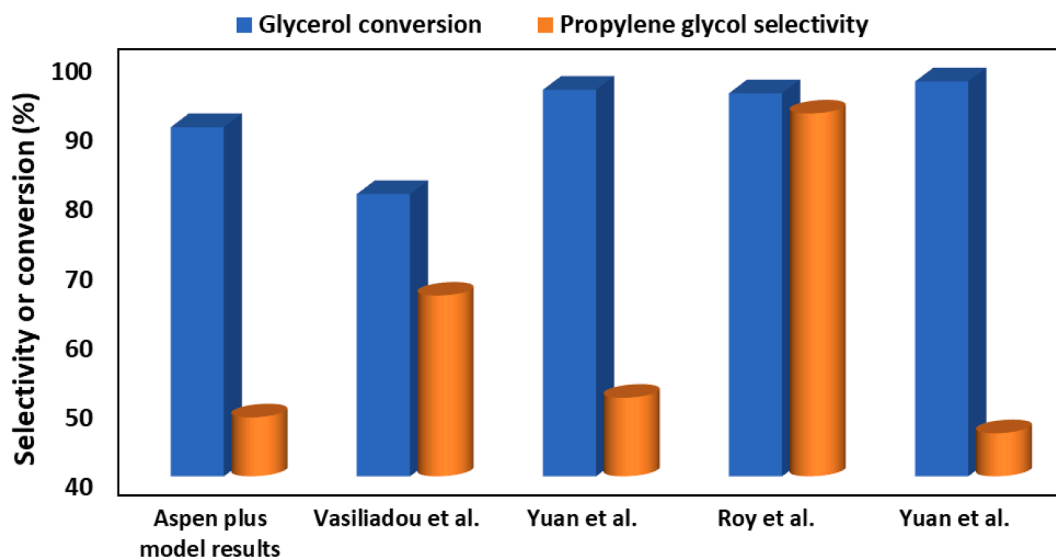


Fig. 3. Comparison of model results with experimental values [36–39].

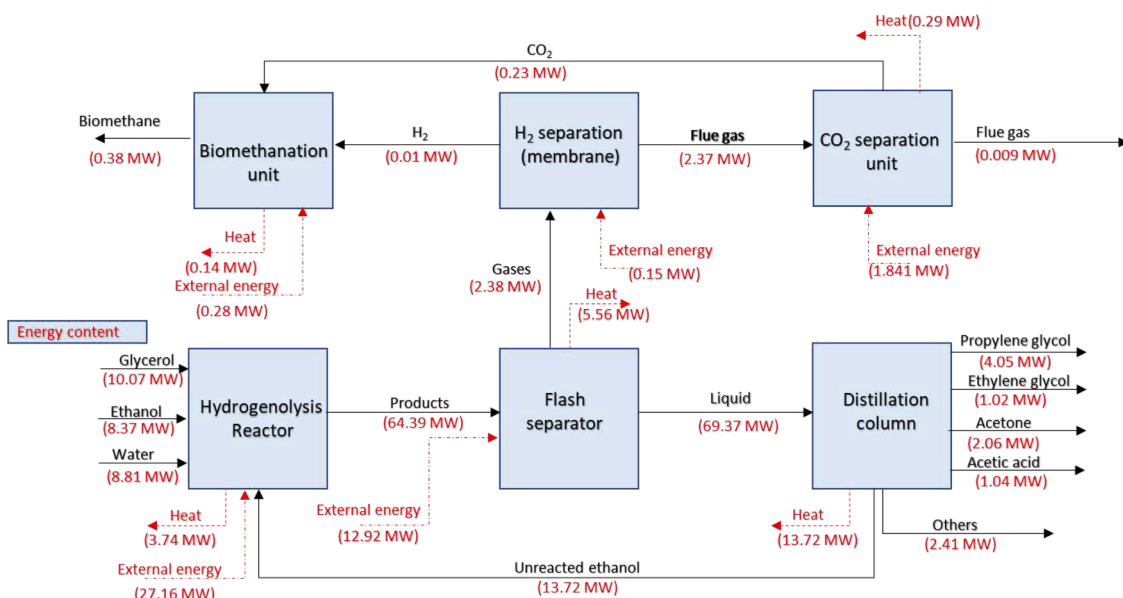


Fig. 4. An overview of the energy balance for the proposed conceptual design.

biomethane and propylene glycol via CTH with CO₂-MEA capture. The energy efficiency obtained for the CTH process is 44.74% and 39.5% for the biomethanation unit. This is in agreement with the energy efficiency reported from a previous study related to catalytic hydrogenolysis [28]. Also, most of the energy expended in the process is from the hydrogenolysis reaction and separation unit due to the series of distillation columns required for high-purity propylene glycol production.

3.2. Economic analysis

3.2.1. Equipment purchase cost, CAPEX and OPEX

The result of the overall equipment purchase cost (EPC) for the integrated CTH process for propylene glycol and biomethane production is shown in Fig. 5a. The cost of the equipment is updated to the current base year 2022 by using the CEPCI. As seen in Fig. 5, the distillation columns accounted for about 66% of the overall EPC. Also, the additional components of the distillation columns such as the condenser, reboiler, and reflux pump are responsible for the cost. In addition, factors like tray type, column height, insulation, and supports are included in the cost estimation of distillation columns. The separators, reactors,

mixers, pumps, and heat exchangers account for 20.47%, 6.65%, 1.47%, 1.46%, and 3.93%, respectively.

Fig. 5b and 5c displays the breakdown of the assessed CAPEX and OPEX. Detailed information about the CAPEX and OPEX appraisal has been documented elsewhere [30,40]. The CAPEX included startup costs (SUC), working capital, and fixed capital expenditure, as illustrated below. While the OPEX was estimated from fixed operating cost, total utility cost, and variable operating cost. The fixed capital investment contributes about 83% of the overall capital expenditures. This is a result of the EPC, piping and electrical systems, yard improvements, indirect cost, etc. On the contrary, the startup cost contributes about 4% of the overall capital expenditures. The fixed operating cost and variable operating cost contribute significantly to the OPEX, which accounts for about 11% and 89%, respectively. The high VOC could be attributed to the cost of utilities and feedstock cost including the biomethanation unit and series of distillation units for separation which takes up a lot of energy. The feedstock used for CTH includes a catalyst and hydrogen donor (ethanol). The increased cost of ethanol, catalyst regeneration and cost of crude glycerol could be responsible for the high VOC. The cost of supervision, maintenance, tax,

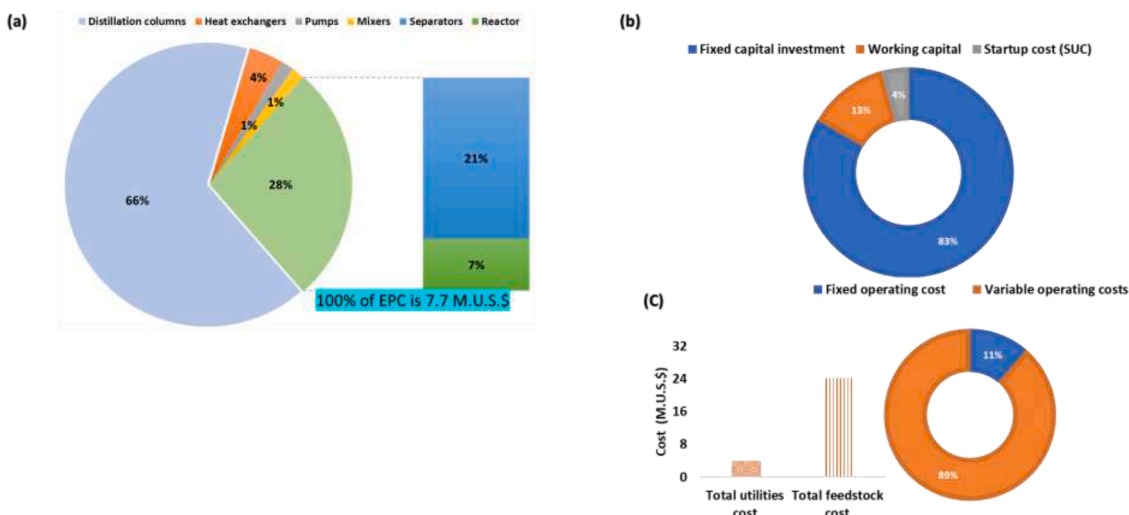


Fig. 5. Breakdown of the (a) Equipment purchase cost (b) Capital expenditure (c) Operating expenditure.

insurance, and other supplemental charges were all included in the fixed operating cost (FOC).

3.2.2. Cash flow analysis

A discounted cash flow analysis (DCFA) was performed to evaluate the MSP of propylene glycol and biomethane produced from the proposed technology. The results of the DCFA are presented in Table 2. The results were compared with a standalone biomethanation plant for biomethanation reaction as well as a catalytic hydrogenolysis plant with external green hydrogen from electrolysis reaction [28]. It should be noted that all cost estimates were different based on varying assumptions used in the model as well as the year of economic evaluation. Regardless, the results reported herein are a good basis for comparison especially when it relates to a conceptual design.

As illustrated in Table 2, the MSP of propylene glycol produced considering the overall cost of biomethane co-product is 1.41 U.S.\$/kg. However, if the cost of biomethane was not considered or if the biomethane produced is not enough to yield a yearly revenue then the MSP would increase to 1.43 U.S.\$/kg. When compared with a standalone CTH process (a process that does not include the biomethanation and capture unit), the MSP of propylene glycol is relatively lower (0.99 U.S.\$/kg). The MSP of propylene glycol from the integrated CTH, CO₂ capture and biomethane reaction was also compared with that from catalytic hydrogenolysis reaction that uses external hydrogen from steam reforming. Catalytic hydrogenolysis reaction had higher MSP (2.9 U.S.\$/kg). The increased MSP could be attributed to the added cost of hydrogen from the steam reforming reaction. The proposed technique is within the range of the business as usual (BAU) route, which uses the

Table 2
The MSP of propylene glycol and biomethane from different processes.

Product	Process	MSP of propylene glycol (U.S. \$/kg)	MSP of biomethane (U.S. \$/MWh)	Refs.
Propylene glycol	CTH, CO ₂ capture and biomethanation (considering the cost of biomethane)	1.41	–	This study
	CTH, CO ₂ capture and biomethanation (without the cost of biomethane)	1.43	–	This study
	Catalytic hydrogenolysis with external hydrogen (steam reforming)	2.9	–	Omoarukhe et al. [28]
	CTH standalone process	0.99	–	Omoarukhe et al. [28]
Biomethane	CTH, CO ₂ capture and biomethanation (considering the cost of biomethane)	–	148	Omoarukhe et al. [28]
	Anaerobic digestion and biomethanation	–	148.90	Okolie et al. [41]
	AD, conventional gasification and biomethanation	–	187.7	Michailos al. [42]
	Hydrothermal gasification with syngas fermentation with carbon capture, electrolysis and biomethanation	–	159.5	Okolie et al. [10]

non-catalytic liquid-phase hydrolysis of propylene oxide (PO), which is still widely used around the world and has a propylene glycol MSP of 1.32 - 1.79 U.S.\$/kg [35].

Biomethane co-product, an MSP of 148 U.S.\$/MWh was obtained. Biomethane MSP is lower than those reported from other integrated processes as shown in Table 2. Therefore, the proposed design could be a promising source of both biomethane and propylene glycol in an integrated biorefinery.

3.2.3. Sensitivity analysis

The main source of uncertainty in the economic analysis for the propylene glycol production process includes ethanol price, CAPEX, tax rate, electricity cost, catalyst cost and EPC. Therefore, sensitivity analysis was performed to identify those with the highest impact on the economic feasibility of the proposed technology. The parameters were varied at ± 30% and the direct impact of the variation on MSP was reported in Fig. 6a and 6b. Ethanol price had the greatest impact on the MSP of biomethane and propylene glycol.

A 30% elevation in the price of ethanol led to an increase in the MSP of propylene glycol to 1.76 U.S.\$/kg and biomethane to 184.7 U.S.\$/MWh. With a 30% decline in the ethanol price, MSP further decreases to 1.06 U.S.\$/kg for propylene glycol and 111.3 U.S.\$/MWh for biomethane.

Since the cost of ethanol hydrogen donor contributes significantly towards the MSP, future processes should focus on investigating a cost-effective hydrogen donor solvent or performing CTH without a hydrogen donor. Although the production of propylene glycol without any external agents might provide an improved process economics, the challenge of identifying a promising bifunctional catalyst is inherent. Also, it is very important to control and identify the reaction kinetics of several intermediate pathways during the catalyst design.

Other factors such as catalyst cost, electricity cost, FCI and EPC also influence the MSP of biomethane and propylene glycol. Although their influence is not significant when compared with the ethanol cost. For instance, the MSP of propylene glycol and biomethane decreases to 1.35 U.S.\$/kg and 141.7 U.S.\$/MWh with a 30% decline in electricity cost. While an increase in the cost of electricity produced led to an elevation in the MSP to 1.48 U.S.\$/kg for propylene glycol and 158.3 U.S.\$/MWh for biomethane. It should be mentioned that most of the electricity cost is incurred from the product separation and biomethanation unit. Such units would require effective heat integration and energy management to improve the energy and electricity requirements. On-site renewable energy generation could also help in attaining a lower electricity price. For instance, solar or wind energy could be dedicated towards electricity generation for the proposed system. The government could also help by providing incentives for renewable energy generation especially biomethane production. These incentives could be in the form of tax credits, renewable heat incentives (RHI) or carbon pricing. For instance, the United Kingdom government introduced the RHI in 2009 as a fee to support the production of renewable heat (Michailos et al., 2019.) Some studies have shown that the introduction of RHI led to a decline in the MSP of biomethane production from anaerobic digestion [42,43][43].

3.3. Environmental assessment

The environmental impact of the proposed conceptual design was appraised by estimating the amount of CO₂ emissions from the inlet and outlet streams of each process. The emissions from the electricity consumption are estimated based on a factor of 0.73 MT of CO₂/MWh [44]. The EPC methods used to determine the emissions for stationary combustion sources were adopted in the determination of the emissions associated with heating utilities as indicated in Eq. (11).

$$N_{CO_2} = f^*HC^*C_{fuel} * \left(\frac{44kgofCO_2}{12kgofC} \right) \quad (11)$$

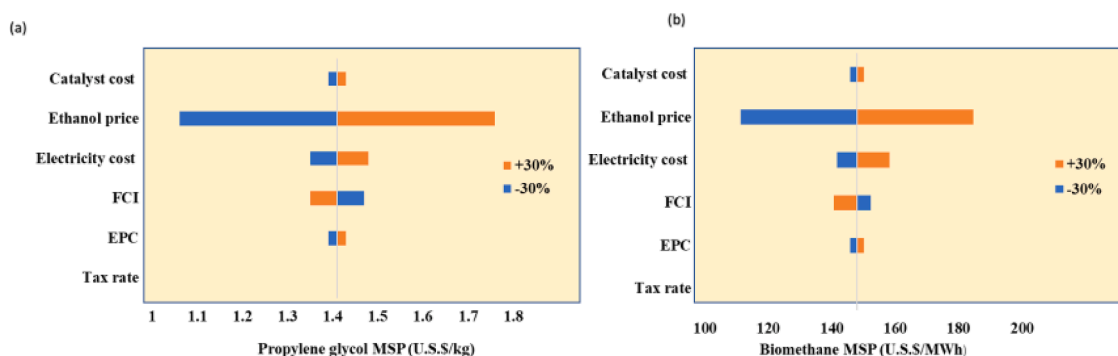


Fig. 6. Sensitivity analysis illustrating the impact of various economic model variables on (a) MSP of propylene glycol (b) MSP of biomethane.

Where F and HC represent the fuel combustion factor and heating content respectively. C_{fuel} is the amount of carbon content in the fuel. NCO_2 is the amount of CO_2 emissions in kg/day.

CO_2 emissions for the proposed CTH and biomethanation reaction as well as the standalone CTH process are presented in Fig. 7. Among the sources of emissions, the emissions related to the use of heating utilities were the highest (3.37 MM tonnes/yr for the integrated process and 3.68 MM tonnes/yr for the standalone process). The superior carbon footprint associated with heating utilities is due to the product separation unit comprising of series of distillation columns required for propylene glycol purification. It should be mentioned that the emission from electricity is higher for the integrated process compared to the standalone CTH due to the additional electricity requirements for the increased unit operations.

However, compared to the integrated process (carbon emissions of 3.5 MM tonnes/yr), the standalone CTH had a higher overall carbon footprint (carbon emissions of 3.7 MM tonnes/yr. This could be attributed to the consumption of CO_2 derived from the process streams via biomethanation process.

4. Conclusions and study limitations

The co-production of biomethane and propylene glycol from waste glycerol has been conceptualised innovatively. The process comprises catalytic transfer hydrogenolysis, CO_2 capture and a biomethanation unit. An economic assessment of the process shows that a biomethane and propylene glycol minimum selling price (MSP) of 149 U.S.\$/MWh and 1.41 U.S.\$/kg were obtained. The price is within the range of the co-products produced commercially through the business-as-usual case. Sensitivity analysis results show that the price of ethanol hydrogen transfer, catalyst cost, electricity and fixed capital investment significantly impact the MSP of both products.

Although the focus of the present study was a preliminary economic

and environmental evaluation of the conceptual design, there are several limitations. In the CO_2 capture unit, a splitter (CSPLITTE unit) was used for the purification of CO_2 since a pure stream is required. The CSPLITTE unit was added as a block because not all of the CO_2 was captured by the MEA. More or less, we need a pure CO_2 Stream, therefore the CSPLITTE was used. Since the focus of the study was a preliminary economic evaluation, a splitter was used. However, in future studies, we need to optimize the CO_2 capture process and perform sensitivity analysis to determine how various factors influence the capture efficiency. MEA- CO_2 absorption was selected as the capture method; however, it would be important to evaluate the cost and performance of different CO_2 capture processes while selecting the most promising technology through a detailed multicriteria analysis. The analysis should consider several factors including the cost and environmental impact.

Funding

The authors did not receive any specific funding for the project. Special thanks to Gallogly College of Engineering, University of Oklahoma, Norman, United states for providing the software tools and facility to complete the research

Declaration of Competing Interest

The authors declare that they have no known competing financial interests or personal relationships that could have appeared to influence the work reported in this paper.

Data availability

Data will be made available on request.

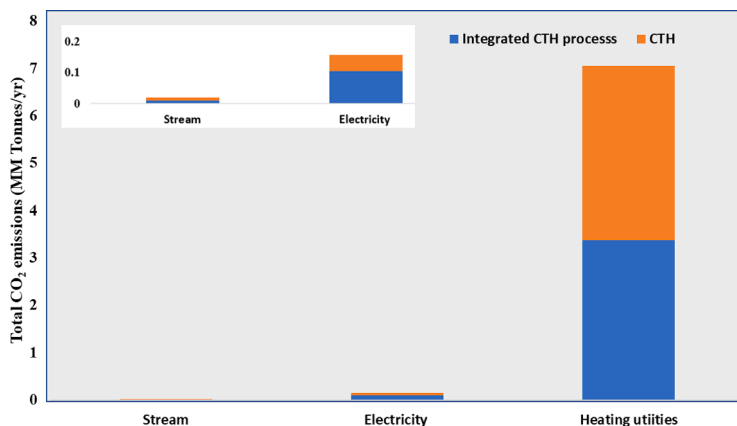


Fig. 7. CO_2 emissions from process streams, electricity utilization and heating utilities. Note that CTH represented a standalone process.

Supplementary materials

Supplementary material associated with this article can be found, in the online version, at [doi:10.1016/j.cej.2023.100523](https://doi.org/10.1016/j.cej.2023.100523).

References

- G. Cican, M. Deaconu, R. Mirea, L. Ceatra, M. Cretu, T. Dobre, Investigating the use of recycled pork fat-based biodiesel in aviation turbo engines, *Processes* 8 (2020) 1196, <https://doi.org/10.3390/PR8091196>.
- J.A. Okolie, J. Ivan Escobar, G. Umenweke, W. Khanday, P.U. Okoye, Continuous biodiesel production: a review of advances in catalysis, microfluidic and cavitation reactors, *Fuel* 307 (2022), 121821, <https://doi.org/10.1016/j.fuel.2021.121821>.
- T. Valliyappan, D. Ferdous, N.N. Bakhshi, A.K. Dalai, Production of hydrogen and syngas via steam gasification of glycerol in a fixed-bed reactor, *Top. Catal.* 49 (2008) 59–67, <https://doi.org/10.1007/s11244-008-9062-7>.
- Y.D. Wang, T. Al-Shemmeri, P. Eames, J. McMullan, N. Hewitt, Y. Huang, et al., An experimental investigation of the performance and gaseous exhaust emissions of a diesel engine using blends of a vegetable oil, *Appl. Therm. Eng.* 26 (2006) 1684–1691, <https://doi.org/10.1016/j.applthermaleng.2005.11.013>.
- R.X. Jiménez, A.F. Young, H.L.S. Fernandes, Propylene glycol from glycerol: process evaluation and break-even price determination, *Renew. Energy* 158 (2020) 181–191, <https://doi.org/10.1016/j.renene.2020.05.126>.
- M.R. Nanda, Z. Yuan, W. Qin, C. Xu, (Charles). Recent advancements in catalytic conversion of glycerol into propylene glycol: a review, *Catal. Rev. Sci. Eng.* 58 (2016) 309–336, <https://doi.org/10.1080/01614940.2016.1166005>.
- J.A. Okolie, Insights on production mechanism and industrial applications of renewable propylene glycol, *IScience* 25 (2022), 104903, <https://doi.org/10.1016/j.isci.2022.104903>.
- P. Sun, W. Zhang, X. Yu, J. Zhang, N. Xu, Z. Zhang, et al., Hydrogenolysis of glycerol to propylene glycol: energy, tech-economic, and environmental studies, *Front. Chem.* 9 (2022), <https://doi.org/10.3389/fchem.2021.778579>.
- J. Zhang, Catalytic transfer hydrogenolysis as an efficient route in cleavage of lignin and model compounds, *Green Energy Environ.* 3 (2018) 328–334, <https://doi.org/10.1016/j.jee.2018.08.001>.
- J.A. Okolie, M.E. Tabat, B. Gunes, E.I. Epelle, A. Mukherjee, S. Nanda, et al., A techno-economic assessment of biomethane and bioethanol production from crude glycerol through integrated hydrothermal gasification, syngas fermentation and biomethanation, *Energy Convers. Manag.* 12 (2021), 100131, <https://doi.org/10.1016/j.ecmx.2021.100131>. X.
- D. Supramono, J.A. Ashshiddiq, Economic potential of the manufacture of acrolein and propylene glycol from glycerol, *AIP Conf. Proc.* 2376 (2021), 020003, <https://doi.org/10.1063/5.0064725>.
- Y.N. Regmi, J.K. Mann, J.R. McBride, J. Tao, C.E. Barnes, N. Labbé, et al., Catalytic transfer hydrogenolysis of organosolv lignin using B-containing FeNi alloyed catalysts, *Catal. Today* 302 (2018) 190–195, <https://doi.org/10.1016/j.cattod.2017.05.051>.
- J. Fang, F. Wu, Y. Xiong, F. Li, H. Yang, S. Wang, et al., Sources of organic matter in the surface sediments from Lake Sihailongwan Maar and Lake Zhanjiang Maar (Lake Huguangyan Maar) in China, *Limnologia* 69 (2018) 18–23, <https://doi.org/10.1016/j.limno.2017.08.004>.
- S. Michailos, S. McCord, V. Sick, G. Stokes, P. Styring, Dimethyl ether synthesis via captured CO₂ hydrogenation within the power to liquids concept: a techno-economic assessment, *Energy Convers. Manag.* 184 (2019) 262–276, <https://doi.org/10.1016/j.enconman.2019.01.046>.
- P. Furda, M. Variny, Z. Labovská, T. Cibulka, Process drive sizing methodology and multi-level modeling linking MATLAB® and Aspen Plus® environment, *Processes* Vol 8 (2020), <https://doi.org/10.3390/PR811495>. Page 1495 202081495.
- D. Zhang, W. Yu, Z. Li, Z. Wang, B. Yin, X. Liu, et al., Strong metal-support interaction of palladium carbide in PtPd/C catalysts for enhanced catalytic transfer hydrogenolysis of glycerol, *Biomass Bioenergy* 163 (2022), 106507, <https://doi.org/10.1016/j.biombioe.2022.106507>.
- E. Sarath Yadav, T. Indiran, D. Nayak, C. Aditya Kumar, M. Selvakumar, Simulation study of distillation column using Aspen plus, *Mater. Today Proc.* 48 (2022) 330–337, <https://doi.org/10.1016/J.MATPR.2020.07.609>.
- F. Sabatino, A. Grimm, F. Gallucci, M. van Sint Annaland, G.J. Kramer, M. Gazzani, A comparative energy and costs assessment and optimization for direct air capture technologies, *Joule* 5 (2021) 2047–2076, <https://doi.org/10.1016/j.joule.2021.05.023>.
- M. Gazzani, E. MacChi, G. Manzolini, CO₂ capture in integrated gasification combined cycle with SEWGS - part a: thermodynamic performances, *Fuel* 105 (2013) 206–219, <https://doi.org/10.1016/j.fuel.2012.07.048>.
- T. Deschamps, M. Kanneche, L. Grandjean, O. Authier, Modeling of vacuum temperature swing adsorption for direct air capture using aspen adsorption, *Clean Technol.* 4 (2022) 258–275, <https://doi.org/10.3390/cleantechnol4020015>.
- A. Kiani, K. Jiang, P. Feron, Techno-economic assessment for CO₂ capture from air using a conventional liquid-based absorption process, *Front. Energy Res.* 8 (2020) 92, <https://doi.org/10.3389/fenrg.2020.00092>.
- C. Alie, L. Backham, E. Croiset, P.L. Douglas, Simulation of CO₂ capture using MEA scrubbing: a flowsheet decomposition method, *Energy Convers. Manag.* 46 (2005) 475–487, <https://doi.org/10.1016/j.enconman.2004.03.003>.
- J. Gaspar, A.M. Cormos, Dynamic modeling and absorption capacity assessment of CO₂ capture process, *Int. J. Greenhouse Gas Control* 8 (2012) 45–55, <https://doi.org/10.1016/j.ijggc.2012.01.016>.
- P. Mores, N. Scenna, S. Mussati, Post-combustion CO₂ capture process: equilibrium stage mathematical model of the chemical absorption of CO₂ into monoethanolamine (MEA) aqueous solution, *Chem. Eng. Res. Des.* 89 (2011) 1587–1599, <https://doi.org/10.1016/j.cherd.2010.10.012>.
- L. Li, M. Maeder, R. Burns, G. Puxty, S. Clifford, H. Yu, The Henry coefficient of CO₂ in the MEA-CO₂-H₂O system, *Energy Procedia* 114 (2017) 1841–1847, <https://doi.org/10.1016/j.egypro.2017.03.1313>.
- K. Li, A. Cousins, H. Yu, P. Feron, M. Tade, W. Luo, et al., Systematic study of aqueous monoethanolamine-based CO₂ capture process: model development and process improvement, *Energy Sci. Eng.* 4 (2016) 23–39, <https://doi.org/10.1002/ese3.101>.
- M. Götz, A.M.D. Koch, F. Graf, State of the art and perspectives of CO₂ methanation process concepts for power-to-gas applications, *Int. Gas Res. Conf. Proc.* 1 (2014) 314–327.
- F.O. Omoarukhe, E.I. Epelle, C.C. Ogbaga, J.A. Okolie, Stochastic economic evaluation of different production pathways for renewable propylene glycol production via catalytic hydrogenolysis of glycerol, *React. Chem. Eng.* (2023), <https://doi.org/10.1039/D2RE00281G>.
- Cost Indices – Towering Skills n.d. <https://toweringskills.com/financial-analysis/cost-indices/> (accessed April 5, 2023).
- A. Mukherjee, J.A. Okolie, C. Niu, A.K. Dalai, Techno – Economic analysis of activated carbon production from spent coffee grounds: comparative evaluation of different production routes, *Energy Convers. Manag.* 14 (2022), 100218, <https://doi.org/10.1016/j.ecmx.2022.100218>. X.
- E.S. Vasiladou, V.L. Yfanti, A.A. Lemonidou, One-pot tandem processing of glycerol stream to 1,2-propanediol with methanol reforming as hydrogen donor reaction, *Appl. Catal. B* 163 (2015) 258–266, <https://doi.org/10.1016/j.apcatb.2014.08.004>.
- I. Gandarias, P.L. Arias, S.G. Fernández, J. Requies, M. el Doukkali, M.B. Güemez, Hydrogenolysis through catalytic transfer hydrogenation: glycerol conversion to 1,2-propanediol, *Catal. Today* 195 (2012) 22–31, <https://doi.org/10.1016/J.CATTOD.2012.03.067>.
- G. Zhang, X. Jin, J. Wang, M. Liu, W. Zhang, Y. Gao, et al., Fe³⁺-mediated Pt/Y zeolite catalysts display enhanced metal–bronsted acid interaction and synergistic cascade hydrogenolysis reactions, *ACS Publ.* 59 (2020) 17387–17398, <https://doi.org/10.1021/acs.iecr.0c01971>.
- X. Liu, B. Yin, W. Zhang, X. Yu, Y. Du, S. Zhao, et al., Catalytic transfer hydrogenolysis of glycerol over heterogeneous catalysts: a short review on mechanistic studies, *Chem. Rec.* 21 (2021) 1792–1810, <https://doi.org/10.1002/TCR.202100037>.
- A. Gonzalez-Garay, M. Gonzalez-Miquel, G. Guillen-Gosalbez, High-value propylene glycol from low-value biodiesel glycerol: a techno-economic and environmental assessment under uncertainty, *ACS Sustain. Chem. Eng.* 5 (2017) 5723–5732, <https://doi.org/10.1021/acsuschemeng.7b00286>.
- J. Yuan, S. Li, L. Yu, Y. Liu, Y. Cao, Efficient catalytic hydrogenolysis of glycerol using formic acid as hydrogen source, *Chin. J. Catal.* 34 (2013) 2066–2074, [https://doi.org/10.1016/S1872-2067\(12\)60656-1](https://doi.org/10.1016/S1872-2067(12)60656-1).
- D. Roy, B. Subramaniam, R.V. Chaudhari, Aqueous phase hydrogenolysis of glycerol to 1,2-propanediol without external hydrogen addition, *Catal. Today* 156 (2010) 31–37, <https://doi.org/10.1016/J.CATTOD.2010.01.007>.
- Vasiladou E., Catalysts A.L., 2014 Undefined. Catalytic glycerol hydrodeoxygenation under inert atmosphere: ethanol as a hydrogen donor. MdpCom n.d.
- C. Cai, C. Zhu, H. Wang, H. Xin, Z. Xiu, C. Wang, et al., Catalytic hydrogenolysis of biomass-derived polyhydric compounds to C₂–C₃ small-molecule polyols: a review, *Curr. Org. Chem.* 23 (2019) 2180–2189, <https://doi.org/10.2174/1385272823666190913185618>.
- J.A. Okolie, S. Nanda, A.K. Dalai, J.A. Kozinski, Techno-economic evaluation and sensitivity analysis of a conceptual design for supercritical water gasification of soybean straw to produce hydrogen, *Bioresour. Technol.* 331 (2021), 125005, <https://doi.org/10.1016/J.BIORTECH.2021.125005>.
- J.A. Okolie, M.E. Tabat, C.C. Ogbaga, P.U. Okoye, P. Davis, B. Gunes, Economic and environmental assessments of a novel integrated process for biomethane production and ammonia recovery from pot ale, *Chem. Eng. J.* 446 (2022), 137234, <https://doi.org/10.1016/J.CEJ.2022.137234>.
- S. Michailos, M. Walker, A. Moody, D. Poggio, M. Pourkashanian, Biomethane production using an integrated anaerobic digestion, gasification and CO₂ biomethanation process in a real waste water treatment plant: a techno-economic assessment, *Energy Convers. Manag.* 209 (2020), 112663, <https://doi.org/10.1016/J.ENCONMAN.2020.112663>.
- S. Michailos, S. McCord, V. Sick, Dimethyl ether synthesis via captured CO₂ hydrogenation within the power to liquids concept: a techno-economic assessment. *GS-E Conversion and*, 2019 Undefined, Elsevier, 2019.
- A.P. Ortiz-Espinoza, M.M.B. Noureldin, M.M. El-Halwagi, A. Jiménez-Gutiérrez, Design, simulation and techno-economic analysis of two processes for the conversion of shale gas to ethylene, *Comput. Chem. Eng.* 107 (2017) 237–246, <https://doi.org/10.1016/J.COMPCHEMENG.2017.05.023>.